

Interface Engineering of High Efficiency Organic-Silicon Heterojunction Solar Cells

Lixia Yang,[†] Yaoping Liu,^{*,†} Wei Chen,[†] Yan Wang,^{†,‡} Huili Liang,[†] Zengxia Mei,[†] Andrej Kuznetsov,[‡] and Xiaolong Du^{*,†}

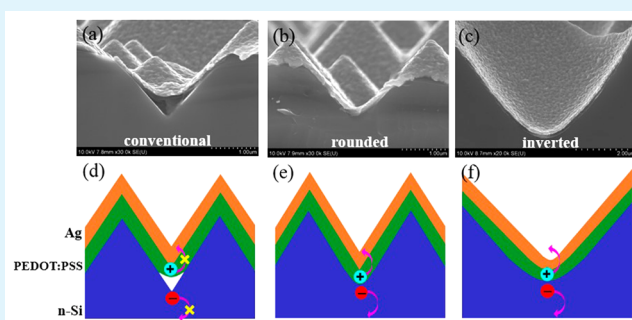
[†]Key Laboratory for Renewable Energy, Beijing Key Laboratory for New Energy Materials and Devices, National Laboratory for Condensed Matter Physics, Institute of Physics, Chinese Academy of Sciences, Beijing 100190, China

[‡]Department of Physics, Centre for Materials Science and Nanotechnology, University of Oslo, PO Box 1048, Blindern, Oslo NO-0316, Norway

S Supporting Information

ABSTRACT: Insufficient interface conformity is a challenge faced in hybrid organic-silicon heterojunction solar cells because of using conventional pyramid antireflection texturing provoking the porosity of interface. In this study, we tested alternative textures, in particular rounded pyramids and inverted pyramids to compare the performance. It was remarkably improved delivering 7.61%, 8.91% and 10.04% efficiency employing conventional, rounded, and inverted pyramids, respectively. The result was interpreted in terms of gradually improving conformity of the Ag/organic/silicon interface, together with the gradually decreasing serial resistance. Altogether, the present data may guide further efforts arising the interface engineering for mastering high efficient heterojunction solar cells.

KEYWORDS: hybrid solar cells, interface conformity, interface engineering, inverted pyramids, light-trapping



Hybrid solar cells based on the composites of poly(3,4-ethylenedioxythiophene):poly(styrenesulfonate) (PEDOT:PSS)/silicon (Si) heterojunction structures are currently attracting significant attention, because of low cost solution-based fabrication and potentially relatively high efficiencies.^{1–5} And a power conversion efficiency of 13.7% has been achieved for the PEDOT:PSS/Si solar cells.⁶ Notably, in the course of the PEDOT:PSS/Si device fabrication, prior to the PEDOT:PSS spin-coating, Si is textured usually in form of nanowires and pyramids to increase the light trapping.^{7–12} Indeed, hybrid solar cells based on random pyramids were demonstrated by Chen et al., permitting low reflectance without introducing severe surface recombination.¹¹ However, a significant amount of air voids remained at the PEDOT:PSS/Si interface in the valleys of the pyramids, resulting in an incomplete interface, which is of great concern on achieving high efficiency of heterojunction solar cells.¹¹ Schmidt et al. also encountered the problem of the partial porosity of the PEDOT:PSS/Si interface as fabricated on the pyramid-textured Si surface and suggested reducing the viscosity of the liquid precursor, which is not an ideal solution.¹² Consequently, it is a critical mission to look after alternative textures combining appropriate light trapping and the interface conformity in order to improve the performance of the PEDOT:PSS/Si hybrid solar cells.

One alternative to improve the PEDOT:PSS/Si interface would be to introduce an additional process to “round” the

valleys of the pyramids, alike to that employed in the HIT (heterojunction with intrinsic thin layer) solar cell processing for better uniformity control of the amorphous Si film as deposited on a conventionally textured crystalline Si substrate.¹³ Moreover, as a result of our recent work, inverted pyramid structures were fabricated by a low-cost one-step metal assisted chemical etching of Si.¹⁴ Importantly, in addition to low reflectivity superiority, these inverted pyramid structures are characterized with rounded and wide deeps, making this texture very applicable for conformal coating and filling, as such in PEDOT:PSS/Si hybrid solar cells.

In this work, we fabricated hybrid solar cells employing these different textures: (i) conventional pyramids, (ii) pyramids with rounded valleys and (iii) inverted pyramids, using otherwise identical processing conditions and materials. Further characterization revealed better performance of (ii) and (iii) on behalf of an exceptional conformity at the PEDOT:PSS/Si and Ag/PEDOT:PSS interface. Importantly, process (iii) resulted in the best cell performance not only resulting from the better interface conformity but also due to superior light trapping as demonstrated earlier.¹⁴

Received: November 12, 2015

Accepted: December 24, 2015

Published: December 24, 2015



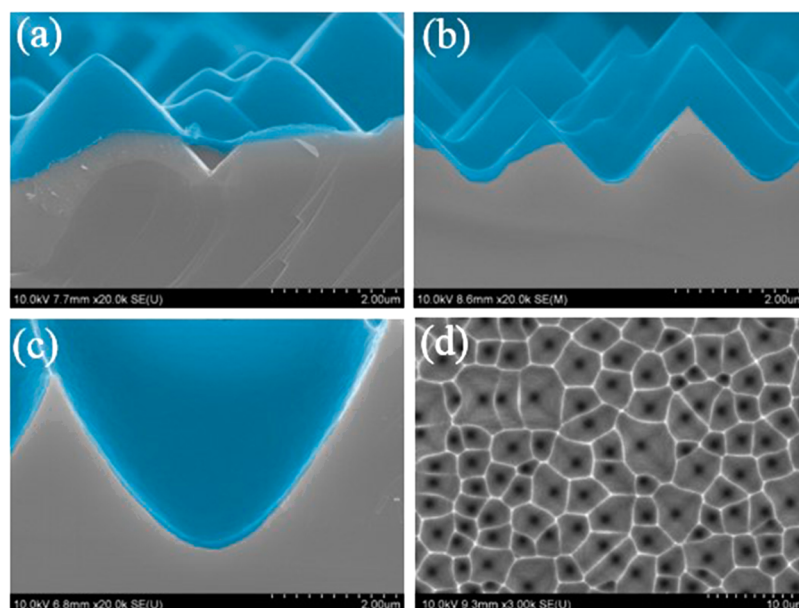


Figure 1. SEM cross-sectional images of the PEDOT:PSS/Si interface employing (a) “conventional” (b) “rounded” and (c) “inverted” pyramid textures. The PEDOT:PSS film is colored in blue for eye guide; (d) SEM top-view image of the inverted pyramid texture.

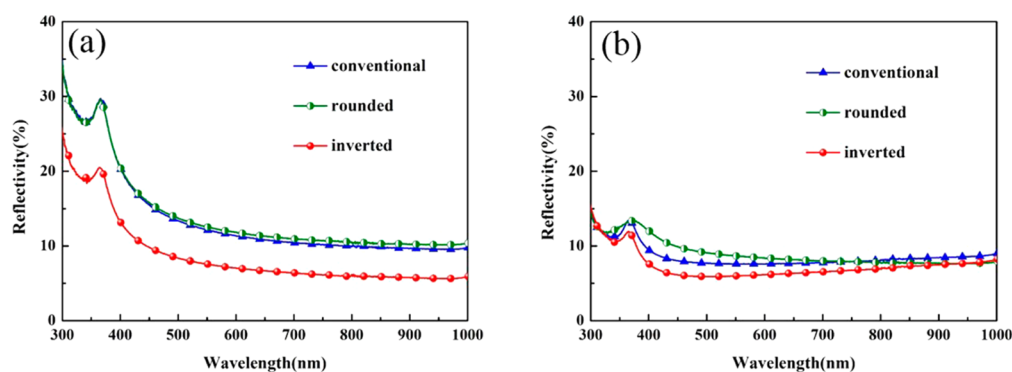


Figure 2. Reflectance spectra of the textured samples (a) before and (b) after PEDOT:PSS spin-coating.

The experimental and devices fabrication methods are discussed in detail in the [Supporting Information](#) (SI). Briefly, these different types of textures were realized on Si substrates, literally in form of (i) conventional pyramids, fabricated by anisotropic etching of Si in an aqueous alkaline solution, (ii) pyramids with rounded valleys, fabricated by isotropic etching of conventional pyramids structured Si in an aqueous solution with HF and HNO₃ and (iii) inverted pyramids, fabricated by maskless Cu-assisted anisotropic etching of Si in an aqueous solution with HF, H₂O₂ and Cu(NO₃)₂, labeled correspondingly as “conventional”, “rounded” and “inverted” samples. Then PEDOT:PSS (PH1000) was mixed with 5 wt % dimethyl sulfoxide (DMSO) to achieve a highly conducting form. Prior to spin coating the PEDOT:PSS layer, the aluminum back electrode was deposited on the precleaned Si substrates. Finally, the silver frontal electrode was deposited on the PEDOT:PSS layer through a shadow mask. A picture of the “inverted” sample after texturing is shown in Figure S1 in the [Supporting Information](#), which exhibits good uniformity. Figure 1a,b,c show the scanning electron microscope (SEM) cross-sectional images of the PEDOT:PSS films as deposited on “conventional”, “rounded” and “inverted” substrates, respectively. The film thickness as may be judged from SEM images, is similar in all samples and is of the order of ~50 nm. However, the

conformity of the interface is apparently different. Indeed, Figure 1a reveals that voids remained in valleys of the conventional pyramid textures, because it is difficult for PEDOT:PSS to go into these narrow valleys during the spin-coating process, thus leading the valleys to be uncovered. Although the conformity of the interface is significantly improved in the “rounded” and “inverted” samples. Figure 1b shows an SEM image of rounded pyramids after secondary etching process, it is obvious that the valleys of the pyramids are becoming open and wide, and the PEDOT:PSS layer conformity is effectively improved. A much wider and opener inverted pyramid structure is exhibited in Figure 1c. Obviously, a conformal coverage of PEDOT:PSS layer down to the bottoms is formed, which indicates a good interface quality of the junction. For a reference, Figure 1d shows the morphology of the inverted pyramid textures prior to the PEDOT:PSS spin-coating.

Further reflectance spectra were recorded to compare light trapping properties of the samples before and after spin-coating of the PEDOT:PSS films, see Figure 2a,b, respectively. One of the prominent trends for the light trapping evolution in Figure 2 is that PEDOT:PSS films act as efficient antireflective coatings, particularly well for the conventional and rounded pyramid textures, whereas the inverted pyramids exhibited

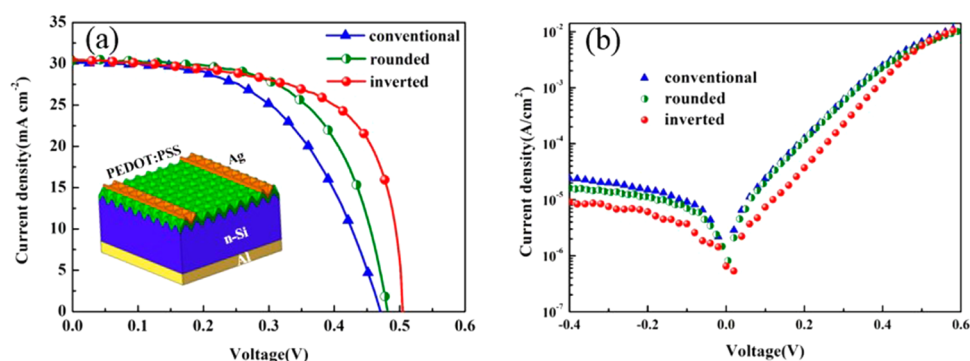


Figure 3. Current density–voltage characteristics of the hybrid solar cells fabricated with different textures (a) under AM1.5 illumination condition and (b) in darkness. The inset shows a schematic illustration of the hybrid solar cells.

Table 1. Characteristics of the Hybrid Solar Cells

sample	V_{oc} (V)	J_{sc} ($\text{mA}\cdot\text{cm}^{-2}$)	FF (%)	PCE (%)	R_s ($\text{ohm}\cdot\text{cm}^2$)	J_0 ($\text{mA}\cdot\text{cm}^{-2}$)	n
conventional	0.472	30.22	53.37	7.61	7.15	2.99×10^{-6}	2.24
rounded	0.484	30.21	60.95	8.91	0.95	2.65×10^{-6}	1.99
inverted	0.504	30.59	65.12	10.04	0.15	0.75×10^{-6}	1.68

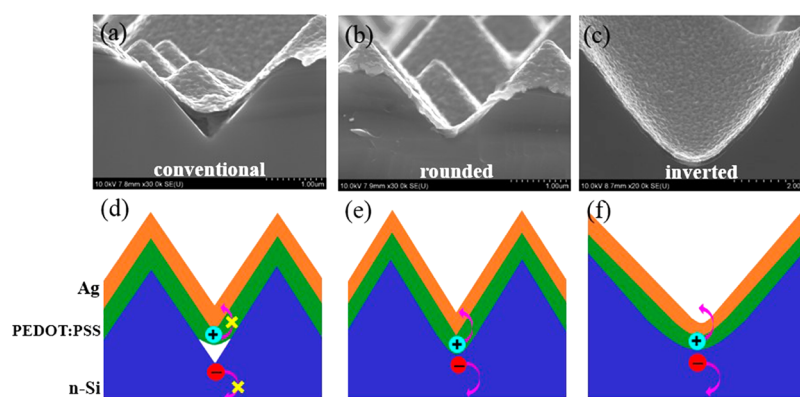


Figure 4. (a–c) Magnified SEM cross-sectional images of Ag/PEDOT:PSS/Si stacks, which panels d–f are the corresponding schematics illustrating carrier transfer in samples with different textures.

minimal reflectivity already initially in accordance with our previous work.¹⁴ Notably, a slight degradation in reflectivity as a result of rounding of the valleys in conventional pyramids, see Figure 2a, indirectly indicates that the rounding treatment was efficient, correlating with the morphology transitions as revealed in Figure 1a,b.

Upon sequential device fabrication processes, hybrid solar cells were characterized under AM 1.5 illumination with an intensity of $100 \text{ mW}/\text{cm}^2$ for evaluating potential efficiency gains as a result of using different textures. Figure 3 shows current density–voltage (J – V) characteristics of these hybrid solar cells under illumination (a) and in darkness (b). As can be deduced from Figure 3a, the open-circuit voltage (V_{oc}), the fill-factor (FF) and the cell efficiency have increased remarkably when changing textures (see Table 1). The reverse saturation current density (J_0) and ideality factor (n) have been extracted from the intercept on the vertical axis from the log (dark current)–voltage graph (Figure 3b), as shown in Table 1. The ideality factors (n) are different for the three samples. This n is used to understand the electronic process in Schottky diodes.³ The values of n decrease when the interface conformity increases from “conventional” to “inverted” samples, suggesting a reduction in carriers recombination. Also, as exhibited in Figure 1 and Table 1, it can be inferred that good interface

conformity can reduce the J_0 . As we know, lower J_0 can lead to higher V_{oc} according to the relationship between V_{oc} and J_0 , thus good interface conformity can improve the V_{oc} . Therefore, according for the data in Figure 1, Figure 3 and Table 1, it may be readily concluded that the performance of these hybrid solar cells is strongly improved with eliminating the porosity at the PEDOT:PSS/Si interface, and Figure 1 provides more insights into the mechanism. It is significantly important to discern the correlation between performance enhancement and conformity of PEDOT:PSS/Si interface, therefore a detailed study is carried out to elucidate the correlation. The schematic models in Figure 4d,e,f illustrate the observed differences in the nature of the interface conformity between the three kinds of textures, with the carriers transfer processes during the cell operation marked by arrows. Specially, for conventional pyramid textures (Figure 4d), the voids occurrence at the PEDOT:PSS/Si interface, are likely to form local shunts, which ultimately deteriorate the V_{oc} and FF of the solar cells.^{11,15,16} In addition, the carriers cannot be separated and transported there and will not contribute to the generation of photocurrent, thus leading to a low current density.¹⁷ As a result, the worst PCE of 7.61% is yielded for “conventional” sample. In its rounding of the deeps in the conventional pyramid texture allows PEDOT:PSS to penetrate down to the deep bottoms (see Figure 4e),

forming a better coverage layer on Si surface, which not only form a sufficient passivated layer on the whole wafer surface, minimizing the interface recombination losses but also increase the areas of the junction, facilitating the carriers separation and transport through the PEDOT:PSS layer.^{15,18,19} Altogether, these improvements deliver a significant efficiency enhancement up to 8.91% primarily on behalf of the V_{oc} and FF increase. Concurrently, the short-circuit current density, J_{sc} does not change much in devices using both types of normal pyramid textures (see Table 1). Importantly, the use of inverted pyramid texturing (Figure 4f) extends the device efficiency up to 10.04% as a result of eliminating the interface porosity problem, demonstrating superior V_{oc} , FF and J_{sc} (see Table 1).

It is worth mentioning that the trend in the serial resistance (R_s) variation correlates with the efficiency increase in Table 1, which is also attributed to the conformity of the Ag/PEDOT:PSS/Si interface as seen from Figure 4a,b,c. It is known that the direct connection between Ag electrode and the emitter region plays a key role in the reduction of R_s .²⁰ Herein, the R_s of our solar cells is significantly influenced by the interface conformity of PEDOT:PSS/Si and Ag/PEDOT:PSS. And, the interface quality of PEDOT:PSS/Si is more critical because the coverage of PEDOT:PSS is very sensitive to the morphology of Si surface while Ag electrode layer prepared by sputtering process usually conformally copies the morphology of the PEDOT:PSS layer. As shown in Figure 4a,d, for “conventional” samples, the photon-generated carriers must travel a longer way in the Si layer before they reach the Ag electrode due to the existence of uncovered region in PEDOT:PSS/Si interface. Some of them will be lost during their trips due to the recombination and cannot be collected by the Ag electrode, leading to the lower current density. In contrast, Figure 4b,c show that there is no shunt in the interface for the “rounded” and “inverted” samples, resulting in more efficiently carriers’ transport and collection as demonstrated in Figure 4e,f.

In summary, a trend of increasing efficiency in the PEDOT:PSS/Si hybrid solar cells as a function of the interface conformity was revealed. As a result, a record high for this type of cells-efficiency of 10.04% is achieved with V_{oc} , J_{sc} , FF, R_s of 504 mV, 30.59 mA/cm², 65.12% and 0.15 ohm·cm², respectively, employing inverted pyramid textures. The influences of interface conformity on the cell performance are carefully investigated. Our results here demonstrate that the performance are positively correlated with the interface conformity, and the open and wide structures such as inverted pyramids are favorable for forming good interface engineering. In addition, the PEDOT:PSS/Si hybrid solar cells based on inverted pyramid structures are very promising for future solar energy conversion.

■ ASSOCIATED CONTENT

Supporting Information

The Supporting Information is available free of charge on the ACS Publications website at DOI: 10.1021/acsami.5b10959.

Methods and an image of Si wafer after inverted pyramid texturing (PDF).

■ AUTHOR INFORMATION

Corresponding Authors

*Y. Liu. Phone: +86-10-82649975. E-mail: ypliu@iphy.ac.cn.

*X. Du. E-mail: xldu@iphy.ac.cn.

Notes

The authors declare no competing financial interest.

■ ACKNOWLEDGMENTS

This work was supported by the Ministry of Science and Technology of China (Grant Nos. 2011CB302002 and 2009CB929404), the National Science Foundation of China (Grant Nos. 11174348, 51272280, 11274366, 61204067 and 61306011), the Chinese Academy of Sciences and the Research Council of Norway in the framework of the IDEAS grant program administrated via the ENERGIX program.

■ REFERENCES

- (1) Jeong, S.; Garnett, E. C.; Wang, S.; Yu, Z.; Fan, S.; Brongersma, M. L.; McGehee, M. D.; Cui, Y. Hybrid Silicon Nanocone–Polymer Solar Cells. *Nano Lett.* **2012**, *12*, 2971–2976.
- (2) Avasthi, S.; Lee, S.; Loo, Y.-L.; Sturm, J. C. Role of Majority and Minority Carrier Barriers Silicon/Organic Hybrid Heterojunction Solar Cells. *Adv. Mater.* **2011**, *23*, 5762–5766.
- (3) Zhang, Y.; Zu, F.; Lee, S.-T.; Liao, L.; Zhao, N.; Sun, B. Heterojunction with Organic Thin Layers on Silicon for Record Efficiency Hybrid Solar Cells. *Adv. Energy Mater.* **2014**, *4*, DOI: 10.1002/aenm.201300923.
- (4) Thomas, J. P.; Zhao, L.; McGillivray, D.; Leung, K. T. High-Efficiency Hybrid Solar Cells by Nanostructural Modification in PEDOT:PSS with Co-Solvent Addition. *J. Mater. Chem. A* **2014**, *2*, 2383–2389.
- (5) He, L.; Lai, D.; Wang, H.; Jiang, C.; Rusli. High-Efficiency Si/Polymer Hybrid Solar Cells Based on Synergistic Surface Texturing of Si Nanowires on Pyramids. *Small* **2012**, *8*, 1664–1668.
- (6) Zhang, Y.; Cui, W.; Zhu, Y.; Zu, F.; Liao, L.; Lee, S.-T.; Sun, B. High Efficiency Hybrid PEDOT:PSS/nanostructured Silicon Schottky Junction Solar Cells by Doping-Free Rear Contact. *Energy Environ. Sci.* **2015**, *8*, 297–302.
- (7) Shen, X.; Sun, B.; Liu, D.; Lee, S.-T. Hybrid Heterojunction Solar Cell Based on Organic–Inorganic Silicon Nanowire Array Architecture. *J. Am. Chem. Soc.* **2011**, *133*, 19408–19415.
- (8) Wang, W.-L.; Zou, X.-S.; Zhang, B.; Dong, J.; Niu, Q.-L.; Yin, Y.-A.; Zhang, Y. Enhanced Photovoltaic Performance of Organic/silicon Nanowire Hybrid Solar Cells by Solution-Evacuated Method. *Opt. Lett.* **2014**, *39*, 3219.
- (9) Wang, J.; Wang, H.; Prakoso, A. B.; Togonal, A. S.; Hong, L.; Jiang, C.; Rusli. High Efficiency Silicon Nanowire/organic Hybrid Solar Cells with Two-Step Surface Treatment. *Nanoscale* **2015**, *7*, 4559–4565.
- (10) Lu, W.; Wang, C.; Yue, W.; Chen, L. Si/PEDOT:PSS Core/shell Nanowire Arrays for Efficient Hybrid Solar Cells. *Nanoscale* **2011**, *3*, 3631–3634.
- (11) Chen, T.-G.; Huang, B.-Y.; Chen, E.-C.; Yu, P.; Meng, H.-F. Micro-Textured Conductive Polymer/silicon Heterojunction Photovoltaic Devices with High Efficiency. *Appl. Phys. Lett.* **2012**, *101*, 033301.
- (12) Schmidt, J.; Titova, V.; Zielke, D. Organic-Silicon Heterojunction Solar Cells: Open-Circuit Voltage Potential and Stability. *Appl. Phys. Lett.* **2013**, *103*, 183901.
- (13) Mishima, T.; Taguchi, M.; Sakata, H.; Maruyama, E. Development Status of High-Efficiency HIT Solar Cells. *Sol. Energy Mater. Sol. Cells* **2011**, *95*, 18–21.
- (14) Wang, Y.; Yang, L.; Liu, Y.; Mei, Z.; Chen, W.; Li, J.; Liang, H.; Kuznetsov, A.; Xiaolong, D. Maskless Inverted Pyramid Texturization of Silicon. *Sci. Rep.* **2015**, *5*, 10843.
- (15) Yu, P.; Tsai, C.-Y.; Chang, J.-K.; Lai, C.-C.; Chen, P.-H.; Lai, Y.-C.; Tsai, P.-T.; Li, M.-C.; Pan, H.-T.; Huang, Y.-Y.; Wu, C.-I.; Chueh, Y.-L.; Chen, S.-W.; Du, C.-H.; Horng, S.-F.; Meng, H.-F. 13% Efficiency Hybrid Organic/Silicon-Nanowire Heterojunction Solar Cell via Interface Engineering. *ACS Nano* **2013**, *7*, 10780–10787.

(16) Pudasaini, P. R.; Ruiz-Zepeda, F.; Sharma, M.; Elam, D.; Ponce, A.; Ayon, A. A. High Efficiency Hybrid Silicon Nanopillar–Polymer Solar Cells. *ACS Appl. Mater. Interfaces* **2013**, *5*, 9620–9627.

(17) Thomas, J. P.; Leung, K. T. Defect-Minimized PEDOT:PSS/Planar-Si Solar Cell with Very High Efficiency. *Adv. Funct. Mater.* **2014**, *24*, 4978–4985.

(18) Thomas, J. P.; Zhao, L.; Abd-Ellah, M.; Heinig, N. F.; Leung, K. T. Interfacial Micropore Defect Formation in PEDOT:PSS-Si Hybrid Solar Cells Probed by TOF-SIMS 3D Chemical Imaging. *Anal. Chem.* **2013**, *85*, 6840–6845.

(19) Wei, W.-R.; Tsai, M.-L.; Ho, S.-T.; Tai, S.-H.; Ho, C.-R.; Tsai, S.-H.; Liu, C.-W.; Chung, R.-J.; He, J.-H. Above-11%-Efficiency Organic–Inorganic Hybrid Solar Cells with Omnidirectional Harvesting Characteristics by Employing Hierarchical Photon-Trapping Structures. *Nano Lett.* **2013**, *13*, 3658–3663.

(20) Zhang, J.; Lee, S.-T.; Sun, B. Effect of Series and Shunt Resistance on Organic-Inorganic Hybrid Solar Cells Performance. *Electrochim. Acta* **2014**, *146*, 845–849.